

Programmable non-volatile spectral shaping in PCM-enhanced grating-assisted couplers

Original

Programmable non-volatile spectral shaping in PCM-enhanced grating-assisted couplers / Tunesi, L., Mahdian, M.A., Shafiee, A., Carena, A., Curri, V., Nikdast, M., Bardella, P.. - ELETTRONICO. - 13362:(2025), pp. 19-23. (SPIE Photonics West - BIOS San Francisco (USA) 25-31 January 2025) [10.1117/12.3044283].

Availability:

This version is available at: 11583/2999644 since: 2025-04-29T11:56:16Z

Publisher:

SPIE

Published

DOI:10.1117/12.3044283

Terms of use:

This article is made available under terms and conditions as specified in the corresponding bibliographic description in the repository

Publisher copyright

SPIE postprint/Author's Accepted Manuscript e/o postprint versione editoriale/Version of Record con

Copyright 2025 Society of PhotoOptical Instrumentation Engineers (SPIE). One print or electronic copy may be made for personal use only. Systematic reproduction and distribution, duplication of any material in this publication for a fee or for commercial purposes, and modification of the contents of the publication are prohibited.

(Article begins on next page)

Programmable non-volatile spectral shaping in PCM-enhanced grating-assisted couplers

Lorenzo Tunesi^a, Mohammad Amin Mahdian^b, Amin Shafiee^b, Andrea Carena^a,
Vittorio Curri^a, Mahdi Nikdast^b, and Paolo Bardella^a

^aDepartment of electronics and telecommunications, Politecnico di Torino, Turin, Italy

^bDepartment of Electrical and Computer Engineering, Colorado State University, Fort Collins, CO, USA

ABSTRACT

We present a novel bandwidth programmable photonic integrated filter enabled by Phase-Change Materials (PCM). PCMs are used to enhance and unlock dynamic and non-volatile spectral shaping in Grating-assisted Contra-Directional Couplers (GACDC). Through the use of chalcogenide PCM, such as Sb₂Se₃, the spectral response of these devices can be programmed beyond the traditional limitations of thermo-optic control, while maintaining identical footprint and similar losses. The device is designed and simulated considering thermal control of the crystallization fraction of the Sb₂Se₃ layer, which is compatible with traditional micro heaters available in standard manufacturing process.

Keywords: Grating Assisted Couplers, Bragg Grating, Add-Drop Filters, Phase Change Materials, Bandwidth flexible,

1. INTRODUCTION

Grating-assisted Contra-Directional Couplers (GACDCs) are a class of versatile photonic integrated components, seeing application as wide band add-drop filters,¹ with the capability of targeting less conventional applications such as multi-channel,² mode-specific³ and polarization asymmetric⁴ multiplexing.

Through precise tailoring of the waveguide geometry and grating structures all these functionalities can be achieved, enhancing their importance as building blocks for Silicon Photonics (SiPh) and in general for all platforms of Photonic Integrated Circuits (PICs).

Despite their numerous promising attributes, GACDCs have some drawbacks, such as large footprint and length, especially when targeting small channel bandwidths,⁵ as well as their dynamic tunability, which is constrained by the Thermo-Optic (TO) and Electro-Optic (EO) effects available on the SiPh platform.

The dynamic control if the GACDC response required modulation and chirping of the effective index of the structure along its length, posing a constraint both on the maximum magnitude (TO/EO limitation) as well as power-efficiency, due to the large footprint that must be excited.

In this work, we propose SiPh compatible Phase-Change Materials (PCM) as an energy efficient and enabling technology to improve the tunability of GACDC. PCM are a class of materials whose amorphous/crystalline fraction can be dynamically changed,⁶ allowing non-volatile and reconfigurable effective index control throughout the waveguide device.

We evaluate the required PCM geometry and optimal material, found to be Sb₂Se₃, and showcase the wider dynamic range available, considering the equivalent TO shift when crystallization/quenching temperatures are provided through a micro-heater structure.

The device and responses are simulated through a variety of techniques, with the main simulation model for the GACDC passive response being validated through experimental results.

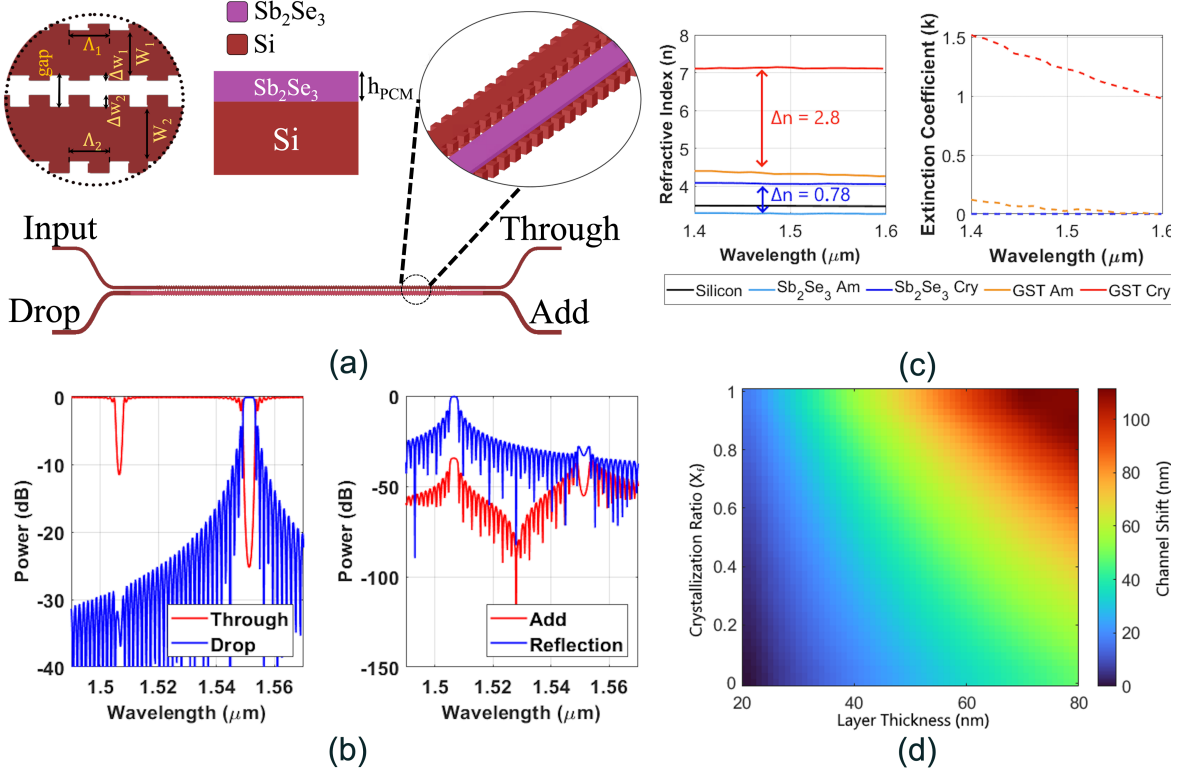


Figure 1: (a) GACDC geometry highlighting the main design parameters as well as the Sb_2Se_3 layer structure. (b) Generic four port response of a GACDC device. (c) Comparison of the refractive index and extinction coefficient of different PCM (Sb_2Se_3 vs $\text{Ge}_2\text{Sb}_2\text{Te}_5$) between their amorphous and crystalline state (Silicon refractive index is also depicted for reference). (d) Channel wavelength shift ($\Delta\lambda$) as a function of PCM thickness (Sb_2Se_3) and crystallization fraction (X_f).

2. DEVICE DESIGN

GACDCs in their straightforward implementation are four-port add-drop filters, leveraging Bragg gratings to introduce frequency-selective coupling in an uncoupled asymmetric waveguides structure. Through the gratings, the forward and backward propagating fields of the waveguides are selectively coupled, resulting in a non-periodic flat-top frequency response.⁷ This response can be shaped through the design of the uncoupled waveguides and the periodic Bragg corrugations geometry, with the widths and pitch affecting the channel wavelength and coupling coefficients. The general schematic of the device can be seen in Fig. 1a, highlighting both the main waveguide parameters, as well as the proposed PCM-loaded geometry: in the following simulations we consider the Sb_2Se_3 layer on top of a single waveguide, although the analysis can be generalized to the case where both waveguides are enhanced with the PCM layer.

Fig. 1b depicts instead the generic response for a GACDC device, depicting the main flat-top channel present at the drop port, as well as the add port crosstalk, through port transmission, and backward reflection.

Parasitic effects, such as intra-waveguide reflection and side-channel ripples, can be minimized through optimal design techniques, like introducing corrugation apodization⁸ to limit the side ripples, and introducing out-of-phase grating to limit the reflection peak.⁹

The geometry of the simulated device considers both these techniques, with an hyperbolic tangent based apodization profile $\Delta w(n) = \frac{\Delta w_{\text{max}}}{2} \left[1 + \tanh \left(\beta \left(1 - 2 \left| \frac{2n-N}{N} \right|^\alpha \right) \right) \right]$, where $\alpha=3, \beta=2$, and n is the index of the period. The waveguides have been simulated with widths $W_1 = 570$ nm and $W_2 = 430$ nm. The coupling gap is 200 nm,

Further author information: (Send correspondence to Lorenzo Tunesi)

Lorenzo Tunesi: E-mail: lorenzo.tunesi@polito.it

and Δw_1 and Δw_2 are 60 nm and 100 nm, respectively. The pitch in considered symmetrical between the waveguides, which are simulated for $n = 2000$ periods, albeit different between the TO control case and the PCM-enhanced structure ($\Lambda_{1,2} = 318$ nm for the T-O device and $\Lambda_{1,2} = 297$ nm for the PCM-based structure): this is necessary to maintain the same central operating wavelength despite the additional Sb_2Se_3 layer, which affects the passive effective index of the device and would lead to a severe central channel shift between the two simulation. The overall effect on the coupling due to the mismatch length is negligible for this study, due to the main focus on the tunability range.

GACDC are typically tuned through TO effects,^{10,11} which can be used to control both the central channel wavelength and its bandwidth. The main disadvantages of TO control are the crosstalk between components, which limits the density of integration, the magnitude of the index shift, which is dictated by the material (Si or SiN) and the low power efficiency, due to the volatile nature of the tuning mechanism. PCMs on the other hand can surpass these limitations, as they provide a larger tuning range while maintaining low power and crosstalk resiliency.

PCMs are characterized by a large shift in optical properties between their crystalline and amorphous state, while stable even in their hybrid state: by controlling their crystallization fraction (X_f) through either thermal or optical means,^{12,13} PCMs can unlock non-volatile programming of the waveguide index, which can be leveraged for many application in PICs.

In this analysis we envision a Sb_2Se_3 layer placed on top of one of the two GACDCs arm, allowing persistent control of the phase-match condition between the coupled mode: the choice of Sb_2Se_3 is due to its advantageous properties with respect to other known PCMs such as $\text{Ge}_2\text{Sb}_2\text{Te}_5$. Fig. 1c depicts the properties of both materials,¹⁴ comparing their refractive index range and extinction coefficient: even though GACDC utilizing $\text{Ge}_2\text{Sb}_2\text{Te}_5$ have been investigated,¹⁵ Sb_2Se_3 is better suited for phase-modulation due to both its lower intrinsic losses ($\text{Ge}_2\text{Sb}_2\text{Te}_5$ exhibit high absorption in the crystalline state) as well as refractive index range compatible to Silicon, which minimizes modal mismatch in both crystalline and amorphous state.

The thickness of the Sb_2Se_3 layer has been designed after simulation of the index shift for different geometries (Fig. 1d): due to the difficulties in achieving precise small-step crystallization control in PCMs, it is important to optimize the geometry based on the desired tunability range. In this analysis we focus on C-band transmission, as such choosing a layer height $h_{\text{PCM}}=50$ nm provide enough range to compare the two control techniques in the whole band.

3. SIMULATION MODELS AND TUNABILITY ANALYSIS

The GACDC has been simulated through a well-established Coupled-Mode Theory (CMT) model.¹⁶ This model has been validated against other simulation techniques such as EigenMode-Expansion (EME) and Finite-Difference Time-Domain (FDTD) methods available in commercial level simulation platform (Ansys Lumerical, Synopsys RSoft), as well as experimental measurement on passive GACDCs realized through electron-beam lithography at Applied Nanotools (Fig. 2a). The CMT model is shown to predict accurate responses in terms of bandwidth and ripples, albeit requiring minor index compensation to match the experimental result central frequency. The fabricated passive GACDCs are affected by channel shift, due to grating smoothing and other

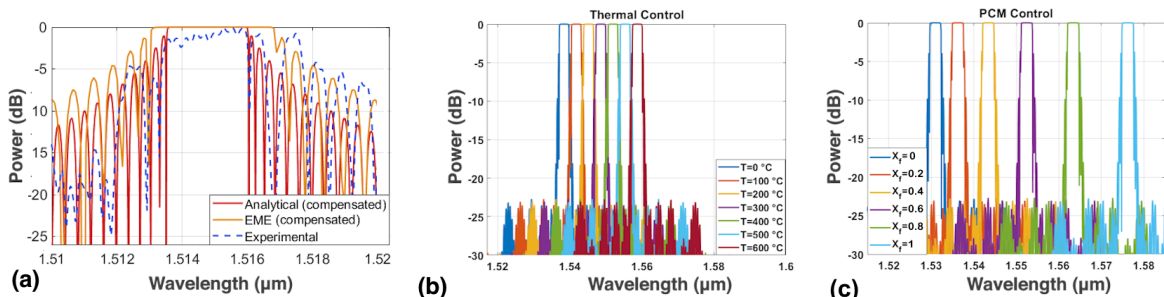


Figure 2: (a) Comparison between CMT model prediction and EME simulations, fitted on the experimental response measurement of a passive SiPh GACDC. (b) Range of channel tunability for the thermally tuned GACDC. (c) Range of channel tunability for the Sb_2Se_3 enhanced GACDC.

non-idealities of the manufacturing process, nonetheless the spectral behavior is shown to be in accordance to the simulation models.

In order to ensure proper comparison between the two control techniques we must consider a temperature profile compatible with the phase-change transition of the chosen material: for Sb_2Se_3 we can consider a crystallization temperature $T_g = 473$ K and a melting temperature $T_l = 884$ K, which has been shown to be achievable through SiPh compatible integrated micro-heater technologies,^{17,18} During the reconfiguration of the PCM layer, the material must be heated to temperatures higher than T_g to induce crystallization, gradually increasing X_f , while switching back to the amorphous state requires melting ($T \geq T_l$) and rapidly cooling the material, leading to quenching.

While longitudinal modulation of the index can be used to achieve control of the channel bandwidth, which was shown to benefit from Sb_2Se_3 -loaded design,¹⁹ in this work we focus on exploring the central channel tunability. Starting from the thermal simulation, and considering Silicon thermo-optic coefficient as $\frac{dn}{dT} = 1.8 \times 10^{-4} \text{ K}^{-1}$, we can simulate the GACDC drop response shift through the CMT model. Considering a temperature bias relative to the ambient temperature in the range $T_l \geq T \geq 0$ the resulting tunability range is shown to be equal to $\Delta\lambda = 20.18$ nm, as shown in Fig. 2b. For the Sb_2Se_3 device, the CMT simulations model the additional PCM layer as index shift for the loaded waveguide. The intermediate values of the refractive index and extinction coefficient for Sb_2Se_3 have been determined through the use of the Lorentz model, extracting the structure effective index through the waveguide geometry simulation.

The tunability effect as a function of the crystallization fraction (X_f) can be seen in Fig. 2c, which highlights a clear increase up to $\Delta\lambda = 45.47$ nm. This result shows not only an twofold improvement in the dynamic tunability of the operating wavelength, but also a severe improvement in power-efficiency. While the power must be continuously applied to the micro-heater to maintain the desired state in the thermal control case, which lead to high power consumption, especially for $T \approx T_l$, the PCM tuning mechanism only requires power during the reconfiguration of the crystallization fraction, with short pulses ($t \leq 1 \times 10^1 \mu\text{s}$) to reach temperatures $T = T_g \approx 473$ K, with the erasing of the state ($X_f = 0$) requiring extremely fast pulses to reach the melting temperature $T \geq T_l = 884$ K.

4. CONCLUSIONS

We demonstrate that Sb_2Se_3 -enhanced GACDCs can overcome the limitations of traditional thermo-optic control, drastically increasing power efficiency. Considering identical temperatures to ensure a valid comparison, we showcase how PCM can be leveraged to extend the tunability range, more than two times the shift achievable through thermo-optic effects. This tuning mechanism can be further extended to reach ranges outside the C-band by increasing the Sb_2Se_3 layer thickness, while maintaining identical tuning scheme. The energy efficiency is drastically improved, only requiring active power during state transition, against the continuous power required by the equivalent thermal tuning scheme.

5. ACKNOWLEDGEMENTS

This work was supported in part by the National Science Foundation (NSF) under grant number CNS-2046226.

REFERENCES

- [1] Hammood, M. et al., “Broadband, silicon photonic, optical add-drop filters with 3 dB bandwidths up to 11 THz,” *Opt. Lett.* **46**, 2738–2741 (6 2021).
- [2] Boroojerdi, M. T. et al., “Two-period contra-directional grating assisted coupler,” *Opt. Express* **24**, 22865–22874 (10 2016).
- [3] Qiu, H. et al., “Silicon mode multi/demultiplexer based on multimode grating-assisted couplers,” *Opt. Express* **21**, 17904–17911 (7 2013).
- [4] Xu, Z. et al., “Compact silicon-based tm-pass/te-divide polarization beam splitter using contra-directional grating couplers assisted by horizontal slot waveguide,” *Optics Communications* **451**, 17–22 (2019).
- [5] Qiu, H. et al., “Narrow-band add-drop filter based on phase-modulated grating-assisted contra-directional couplers,” *J. Lightwave Technol.* **36**, 3760–3764 (9 2018).

- [6] Shafiee, A., Pasricha, S., and Nikdast, M., “A survey on optical phase-change memory: The promise and challenges,” *IEEE Access* **11**, 11781–11803 (2023).
- [7] Shi, W., Wang, X., Lin, C., Yun, H., Liu, Y., Baehr-Jones, T., Hochberg, M., Jaeger, N. A. F., and Chrostowski, L., “Silicon photonic grating-assisted, contra-directional couplers,” *Opt. Express* **21**, 3633–3650 (2 2013).
- [8] Shi, W., Yun, H., Lin, C., Flueckiger, J., Jaeger, N. A. F., and Chrostowski, L., “Coupler-apodized bragg-grating add-drop filter,” *Opt. Lett.* **38**, 3068–3070 (Aug 2013).
- [9] Shi, W. et al., “Single-band add-drop filters using anti-reflection, contra-directional couplers,” in [*The 9th International Conference on Group IV Photonics (GFP)*], 21–23 (2012).
- [10] Tunesi, L., Mahdian, M. A., Carena, A., Curri, V., Nikdast, M., and Bardella, P., “Segmented design and control in contra-directional coupler for large bandwidth tunability,” in [*Optical Components and Materials XXI*], **12882**, 52–57, SPIE (2024).
- [11] Mahdian, M. A. et al., “Bandwidth-adaptive single- and double-channel silicon photonic contra-directional couplers,” in [*IPC*], (2023).
- [12] Ríos, C., Stegmaier, M., Hosseini, P., Wang, D., Scherer, T., Wright, C. D., Bhaskaran, H., and Pernice, W. H. P., “Integrated all-photonic non-volatile multi-level memory,” *Nature Photonics* **9**, 725–732 (11 2015).
- [13] Aryana, K. et al., “Optical and thermal properties of Ge₂Sb₂Te₅, Sb₂Se₃, and Sb₂S₃ for reconfigurable photonic devices,” *Opt. Mater. Express* **13**, 3277–3286 (11 2023).
- [14] Ríos, C. et al., “Ultra-compact nonvolatile phase shifter based on electrically reprogrammable transparent phase change materials,” *Photonix* **3**(1), 26 (2022).
- [15] Hu, H. et al., “Contra-directional switching enabled by Si-GST grating,” *Opt. Express* **28**, 1574–1584 (1 2020).
- [16] Weber, J.-P., “Spectral characteristics of coupled-waveguide Bragg-reflection tunable optical filter,” *IEE Proceedings J (Optoelectronics)* **140**, 275–284(9) (10 1993).
- [17] Fang, Z., Chen, R., Zheng, J., Khan, A. I., Neilson, K. M., Geiger, S. J., Callahan, D. M., Moebius, M. G., Saxena, A., Chen, M. E., Rios, C., Hu, J., Pop, E., and Majumdar, A., “Ultra-low-energy programmable non-volatile silicon photonics based on phase-change materials with graphene heaters,” *Nature Nanotechnology* **17**, 842–848 (Aug 2022).
- [18] Shafiee, A. et al., “Design space exploration for PCM-based photonic memory,” in [*ACM GLSVLSI*], 533–538 (2023).
- [19] Tunesi, L. et al., “Unlocking versatile and non-volatile bandwidth tunability in silicon photonic contra-directional-coupler-based filter devices,” in [*50th European Conference on Optical Communications (ECOC 2024)*], (2024).